Journal of Zhejiang University-SCIENCE A (Applied Physics & Engineering)
ISSN 1673-565X (Print); ISSN 1862-1775 (Online)
www.jzus.zju.edu.cn; link.springer.com
E-mail: jzus_a@zju.edu.cn

A deep energy method for functionally graded porous beams

Arvin MOJAHEDIN[1], Mohammad SALAVATI[2], Timon RABCZUK[†‡3,4]

[1]*Institute of Structural Mechanics, Bauhaus-Universität Weimar, Weimar 99423, Germany*

[2]*Institute of Material Science and Technology, Department of Materials Engineering, Technische Universität Berlin, Berlin 10623, Germany*

[3]*Division of Computational Mechanics, Ton Duc Thang University, Ho Chi Minh City, Vietnam*

[4]*Faculty of Civil Engineering, Ton Duc Thang University, Ho Chi Minh City, Vietnam*

[†]E-mail: timon.rabczuk@tdtu.edu.vn

Received July 18, 2020; Revision accepted Aug. 4, 2020; Crosschecked May 17, 2021

Abstract: We present a deep energy method (DEM) to solve functionally graded porous beams. We use the Euler-Bernoulli assumptions with varying mechanical properties across the thickness. DEM is subsequently developed, and its performance is demonstrated by comparing the analytical solution, which was adopted from our previous work. The proposed method completely eliminates the need of a discretization technique, such as the finite element method, and optimizes the potential energy of the beam to train the neural network. Once the neural network has been trained, the solution is obtained in a very short amount of time.

Key words: Energy-based method; Multilayer perceptron methodology; Functionally graded porous materials; Euler-Bernoulli beam theory

https://doi.org/10.1631/jzus.A2000317 **CLC number:** O313

1 Introduction

Porous materials have extensively been used in engineering owing to their remarkable properties, such as their lightweight nature, large specific surface, flexibility, and high resistance to crack propagation. These materials are commonly used in foams, sound absorption, heat insulation, and electrical applications (Altenbach and Ochsner, 2010). Functionally graded porous materials (FGPMs) are heterogeneous and have various properties that can be modeled by specific continuous functions (Nguyen et al., 2017; Phung-Van et al., 2017, 2019; Thanh et al., 2018, 2019). They have been used in mechanical structures such as beams. Numerical methods to analyze such beams include the finite element method (FEM), Rayleigh-Ritz method, finite difference method, and boundary element method. Numerous studies have examined the behavior of functionally graded material (FGM) beams using different theories. For example, Sankar (2001) analyzed a functionally graded (FG) beam imposed on transverse loads, in which the obtained displacement and stress fields of the FG beam were compared with homogeneous beams. Li et al. (2002) analyzed buckling and post buckling behavior of elastic rods subjected to thermal loads and solved the nonlinear equilibrium equations of Euler-Bernoulli beams using the shooting method. Mojahedin et al. (2018) presented an exact solution of functionally graded porous (FGP) beams under in-plane thermal loading condition using an energy-based method

‡ Corresponding author
ORCID: Arvin MOJAHEDIN, https://orcid.org/0000-0002-2333-5984; Timon RABCZUK, https://orcid.org/0000-0002-7150-296X

assuming a power-law composition for the constituents and considering both saturated and unsaturated pores. Galeban et al. (2016) studied the free vibration of FG thin beams composed of saturated porous materials. The nonlinear equations of motion were derived using a variational formulation based on the Euler-Bernoulli beam theory. The natural frequencies of the FGPM beam were analytically obtained for different boundary conditions. Moreover, they quantified the effects of poroelastic parameters and pore compressibility on natural frequencies. Chen et al. (2016) investigated the free and forced vibration characteristics of FGPM Timoshenko beams subjected to different loads, including a harmonic point load, impulsive point load, and moving load with constant velocity. The equation of motion was discretized using FEM (using the commercial software package ANSYS) in space, and the Newmark-β method was employed for time discretization. Alshorbagy et al. (2011) used FEM to discretize the FGM beam. The large displacement behavior of tapered cantilever beams composed of FG materials under end force conditions was investigated by Nguyen (2014). Chakraverty and Pradhan (2016) analyzed the free vibration of beams composed of FGMs under different boundary conditions based on classical and first-order shear deformation beam theories. They obtained the governing equations using the Rayleigh-Ritz method. Ghannadpour et al. (2013) investigated the bending, buckling, and vibration of nonlocal Euler beams. They used the Ritz method to analyze nonlocal beams under four classical boundary conditions. Their results demonstrated the effectiveness of the Ritz method for modeling nonlocal beams.

Solving differential equations using deep learning methods includes the advantages of lower computational cost, easy training, and parallel computing (Tran-Ngoc et al., 2019; Khatir et al., 2020; Nguyen-Le et al., 2020). Numerous studies have used deep learning solutions for partial differential equations (PDEs). Liu et al. (2019) solved differential equations based on a multilayer feedforward neural network. They presented an neural network model with a combination of a boundary term and multilayer feedforward network. This model improved the accuracy and satisfied the boundary conditions. Nabian and Meidani (2018) used a deep learning approach to solve ordinary differential equation (ODE)/PDE of diffusion and heat conduction problems. They approximated the problems by applying the variation of parameters of a residual neural network. Anitescu et al. (2019) solved second-order boundary value problems using a feedforward fully connected (FC) deep network and adaptive collocation strategy. They used an adaptive approach to select collocation points based on the residual value of the previous training steps. This method improved the robustness of the collocation method in cases of non-smooth regions.

Sirignano and Spiliopoulos (2018) considered Hamilton-Jacobi-Bellman PDE and Burgers' equation by approximating a deep neural network (DNN) solution. They presented an algorithm that combined the Galerkin method and deep learning neural network. The deep learning neural network was trained to satisfy the differential operator and initial and boundary conditions. Shirvany et al. (2009) obtained PDE and ODE equation solutions using multilayer perceptron (MLP) methods. The algorithm was validated by analytical solutions and two well-known numerical methods, i.e., Runge-Kutta method and FEM. The algorithm results showed high accuracy, fast convergence, and low memory usage to solve differential equations. Lagaris et al. (1998) studied the deep learning method to solve initial and boundary value problems. Their scheme used adjustable parameters (weights) in the network only for PDEs, and boundary conditions were not updated during the training. The results of the method were compared with solutions obtained using the Galerkin FEM for several cases of PDEs. Weinan and Yu (2018) used the deep learning method to numerically solve variational problems, particularly those occurring from PDEs. They used variational energy as an objective function to optimize the neural network. They demonstrated that this approach yields appealing visual results, and a short empirical convergence analysis was performed.

In this study, we propose a deep energy method (DEM) for FGP beams based on the Euler-Bernoulli theory to solve the nonlinear strain-displacement relations. Therefore, a loss function, which is the potential energy of the system, is minimized using the Adam optimizer. Boundary conditions are imposed using the penalty method. The method is implemented in PyTorch.

2 Deep energy method

DNN predicts the nonlinear relationship between input and output variables. We use a feedforward DNN by employing the deep learning technique (Fig. 1). Feedforward networks comprise an input (x) layer, hidden layers (H), and an output layer ($Y(x)$). At a given layer, the input from the previous layer is mapped to a neuron through the corresponding weights and biases. MLP employs some form of gradient descent for training (updating the weights and bias) using the backward propagation algorithm, in which large gradients indicate a fast training process. During training, once the loss function is minimized, the weights (θ) and biases (b) are stored as a set of connections.

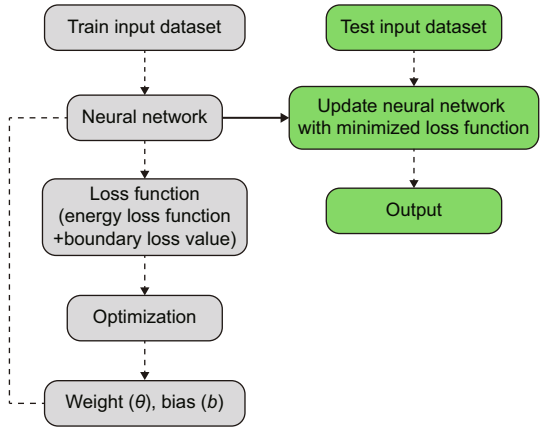

Fig. 1 General supervised learning algorithm

2.1 Neural network architecture

The network architecture is essential. In this study, it is constructed by batching three blocks, in which each block comprises two FC linear transformations, two nonlinear activation functions (AFs), and a residual connection (Fig. 2). The output of each block is vectors in $\mathbb{R}^m$. For a given input vector $\boldsymbol{x}_j = (x_1, x_2, \ldots, x_n)$, the output of the network can be expressed as (Weinan and Yu, 2018):

$$\boldsymbol{Y}_\theta(\boldsymbol{x}) = \mathrm{Block}_1 \mathrm{Block}_2 \cdots \mathrm{Block}_N \cdots \mathrm{FC}, \tag{1}$$

$$\mathrm{FC}_i = \sum_{j=1}^{n} \theta_{ij} x_j + b_i, \tag{2}$$

$$\mathrm{Block}_N = \phi\left(\sum_{j=1}^{n} \theta_{(i+1)j} \phi(\mathrm{FC}_i)_j + b_{(i+1)} \right), \tag{3}$$

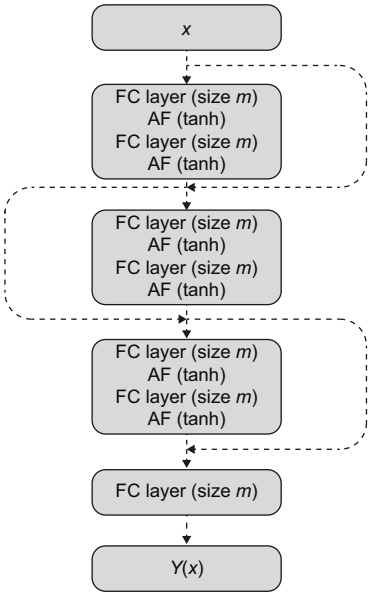

Fig. 2 DNN network with three blocks and a linear output layer (FC). Each block consists of two FC layers and two nonlinear AFs

$$\phi(\mathrm{FC}_i) = \tanh(\mathrm{FC}_i) = \frac{\exp^{\mathrm{FC}_i} - \exp^{-\mathrm{FC}_i}}{\exp^{\mathrm{FC}_i} + \exp^{-\mathrm{FC}_i}}, \tag{4}$$

where ϕ is the nonlinear AF, n the number of training points, FC_i the ith FC layer, and Block_N the Nth output block (Goodfellow et al., 2016). The number of updated parameters (Pa) in each layer is calculated as

$$\mathrm{Pa} = n_{\mathrm{in}} \times n_{\mathrm{out}} + n_{\mathrm{out}}, \tag{5}$$

where n_{in} and n_{out} denote the number of neurons in sequentially connected layers.

2.2 Energy method and loss function

Let us consider a FGP beam with a rectangular cross section under distributed loading condition. The graded properties are assumed to vary through the direction of the thickness (z-axis). The length, width, and height of the beam are denoted by l, s, and h, respectively (Fig. 3).

2.2.1 Functionally graded Euler beam

Let us consider the Euler-Bernoulli theory. The stress-strain (σ-ε) relation and kinematic equations are given as

$$\sigma_{xx} = E(z)\varepsilon_{xx}, \tag{6}$$

$$\varepsilon_{xx} = \frac{\mathrm{d}u(x)}{\mathrm{d}x} + \frac{1}{2}\left(\frac{\mathrm{d}w(x)}{\mathrm{d}x}\right)^2 - z\frac{\mathrm{d}^2 w(x)}{\mathrm{d}x^2}, \tag{7}$$

where $u(x)$ and $w(x)$ denote the displacements in x (axial) and z directions, respectively. The porous material has a nonlinear symmetric porosity distribution along the thickness. The elastic modulus E is assumed to be a function of z (Galeban et al., 2016):

$$E(z)=E_0\left[1-e\cos\left(\frac{\pi z}{l}\right)\right], \tag{8}$$

$$e=1-\frac{E_1}{E_0}, \tag{9}$$

where e is the beam porosity coefficient ($0<e<1$), and E_1 and E_0 the elastic moduli at $z=-h/2$ and $z=h/2$, respectively.

2.2.2 Variation formulation

The total potential energy V is the sum of strain energy U and the potential energy of the applied load W:

$$V=U+W, \tag{10}$$

$$U=\frac{1}{2}\int_v(\sigma_{xx}\varepsilon_{xx})\mathrm{d}v, \tag{11}$$

$$W=-\int_x q(x)w(x)\mathrm{d}x, \tag{12}$$

where v is the volume, and $q(x)$ indicates the distributed load. In our examples, we consider distributed load of the form

$$q(x)=q_0\sin\left(\pi\frac{x}{l}\right). \tag{13}$$

By substituting Eqs. (6) and (7) into Eq. (11), the following expression for V is obtained:

$$V=\frac{1}{2}\int_v E(z)\left[\frac{\mathrm{d}u(x)}{\mathrm{d}x}+\frac{1}{2}\left(\frac{\mathrm{d}w(x)}{\mathrm{d}x}\right)^2-z\frac{\mathrm{d}^2w(x)}{\mathrm{d}x^2}\right]^2\mathrm{d}v-\int_x q(x)w(x)\mathrm{d}x. \tag{14}$$

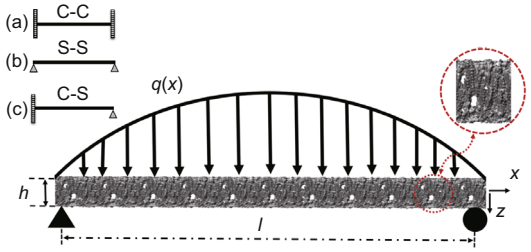

Fig. 3 Geometry system of an FGPM beam under external distributed loading condition $q(x)$, where (a), (b), and (c) denote the clamped-clamped (C-C), simply-simply (S-S), and clamped-simply (C-S) supported boundary conditions, respectively

Integrating with respect to z ($-h/2$ to $h/2$) and y ($-s/2$ to $s/2$) yields the total potential energy:

$$V=\int_x F\left(u,w,\frac{\mathrm{d}u}{\mathrm{d}x},\frac{\mathrm{d}w}{\mathrm{d}x},\frac{\mathrm{d}^2w}{\mathrm{d}x^2};x\right)\mathrm{d}x. \tag{15}$$

2.2.3 Boundary conditions

We considered three types of boundary conditions: simply-simply supported, clamped-clamped, and clamped-simply supported (Fig. 3).

1. Simply-simply support

$$Y(0)=\begin{bmatrix} w(0)\\ M_x(0)\end{bmatrix}=\begin{bmatrix}0\\0\end{bmatrix},$$

$$Y(l)=\begin{bmatrix} w(l)\\ M_x(l)\end{bmatrix}=\begin{bmatrix}0\\0\end{bmatrix}, \tag{16}$$

where the beam moment is expressed as stress variation through the thickness based on the Euler-Bernoulli beam theory:

$$M_x(x)=\int_{-\frac{h}{2}}^{\frac{h}{2}}\sigma_{xx}z\mathrm{d}z. \tag{17}$$

2. Clamped-clamped support

$$Y(0)=\begin{bmatrix} w(0)\\ \frac{\mathrm{d}w(0)}{\mathrm{d}x}\end{bmatrix}=\begin{bmatrix}0\\0\end{bmatrix},$$

$$Y(l)=\begin{bmatrix} w(l)\\ \frac{\mathrm{d}w(1)}{\mathrm{d}x}\end{bmatrix}=\begin{bmatrix}0\\0\end{bmatrix}. \tag{18}$$

3. Clamped-simply support

$$Y(0)=\begin{bmatrix} w(0)\\ \frac{\mathrm{d}w(0)}{\mathrm{d}x}\end{bmatrix}=\begin{bmatrix}0\\0\end{bmatrix},$$

$$Y(l)=\begin{bmatrix} w(l)\\ M_x(l)\end{bmatrix}=\begin{bmatrix}0\\0\end{bmatrix}. \tag{19}$$

2.2.4 Loss function and optimization

DEM is based on minimizing a loss function, which comprises Eq. (15) and boundary terms (Eqs. (16)–(19)), guaranteeing the fulfillment of essential boundary conditions:

$$\mathrm{OF}=\int_x F\left(u,w,\frac{\mathrm{d}u}{\mathrm{d}x},\frac{\mathrm{d}w}{\mathrm{d}x},\frac{\mathrm{d}^2w}{\mathrm{d}x^2};x\right)\mathrm{d}x+h(Y_L,Y_0), \tag{20}$$

where $h(Y_L,Y_0)$ corresponds to the functional boundary conditions. Substituting the full n-layer

network Eq. (1) into Eq. (20) yields the loss function (OF) in terms of the weights (θ) and biases (b). Essential boundary conditions are imposed with the penalty method, as previously mentioned. Using the rectangle rule to evaluate the integrals in Eq. (20) finally yields the following objective function:

$$\mathrm{OF}=\frac{1}{n_{\mathrm{d}}}\sum_{j=1}^{n_{\mathrm{d}}}F_j(\theta,b)+\frac{\beta}{n_{\mathrm{b}}}\sum_{i=1}^{n_{\mathrm{b}}}[h_i(\theta,b)-h_i(Y_L,Y_0)]^2, \tag{21}$$

where n_{d} and n_{b} are the numbers of collocation points in the domain and at the (essential) boundary, respectively, and β is the penalty parameter. The second term on the right hand side of Eq. (21) corresponds to the sum of squared distances between the actual/target values ($h_i(Y_L,Y_0)$) refer to Eqs. (16)–(19) and predicted ($h_i(\theta,b)$) values.

The optimization process minimizes the objective function with respect to weights (θ) and biases (b). We used the Adam optimizer (Kingma and Jimmy, 2015), which is based on the stochastic gradient descent method and readily available in PyTorch.

3 Results and discussion

Let us consider the FGP beam with three types of boundary conditions (Fig. 3). The material parameters are listed in Table 1.

Table 1 FGPM beam properties

Parameter	Value
E_0 (Pa)	1.0×10^9
e	0.5
l (m)	1.00
h (m)	0.01
q_0 (Pa·m)	1.0×10^3

To design an effective network, we stacked six FC layers with skip/residual connections linked at their end with pure FC linear layer (Fig. 2). The training dataset comprises equally distanced 1000 points on the solution domain, while the testing dataset comprises different 100 points:

$$\boldsymbol{x}_{\mathrm{Train}}=[0,\ 0.001,\ldots,\ 1], \tag{22}$$

$$\boldsymbol{x}_{\mathrm{Test}}=[0,\ 0.01,\ldots,\ 1]. \tag{23}$$

The number of each hidden layer (n_{out}) includes 150 neurons, and the output layers include a dataset ($\boldsymbol{w}$), which equals the number of input dataset (n). During training, the updating rate of weights refers to the step size or learning rate (η), which is an important hyper-parameter when configuring the neural network. It controls the pace at which the model is adapted to the problem. We select a learning rate of $\eta=0.015$ with 100 training approaches.

The residual network is often easier to optimize than the FC network. The block-to-block skipping simplifies the network's performance. By increasing the impact of gradients, the learning speed is increased, which leads to better results because there are fewer layers to propagate in the initial training stages. The relative errors obtained from this network architecture and FC neural network are compared in Table 2. By increasing the number of hidden layers and using a deeper network, the relative errors in the residual network decrease. The relative error (R_{e}) is defined as

$$R_{\mathrm{e}}=\parallel(w(x)-w(x)_{\mathrm{exact}})\parallel_2, \tag{24}$$

where $w(x)_{\mathrm{exact}}$ and $w(x)$ are the exact and predicted solutions of the FGP beam's deflection, respectively.

Table 2 Relative error of FC and residual networks

Number of layers	Boundary condition	R_{e} (%)	
		Fully connected	Residual connected
6	S-S	4.228	4.222
6	C-C	3.520	3.496
6	C-S	1.490	1.479
8	S-S	3.382	2.533
8	C-C	2.816	2.098
8	C-S	1.192	0.887
10	S-S	3.044	1.520
10	C-C	2.534	1.260
10	C-S	1.073	0.532
12	S-S	2.739	0.912
12	C-C	2.280	0.756
12	C-S	0.966	0.319

Fig. 4 compares the solution of DEM with the exact solution for clamped-clamped and simply-simply boundary conditions. Notably, the accuracy can be improved by increasing the number of blocks in Fig. 2 and the size of the input dataset. Fig. 5 compares the predicted and exact solutions for the clamped-simply boundary condition. Changing the boundary conditions insignificantly affects the accuracy.

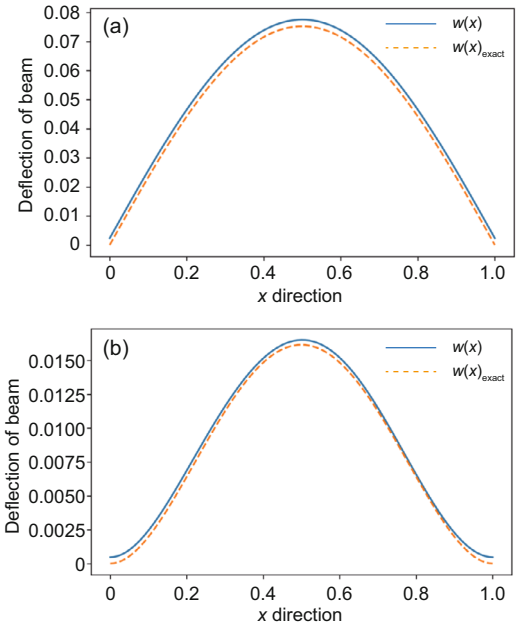

Fig. 4 Comparison of the exact ($w(x)_{\text{exact}}$) (Reddy, 2017) and our predicted ($w(x)$) solution results of residual network with six layers for simply-simply (a) and clamped-clamped (b) boundary conditions

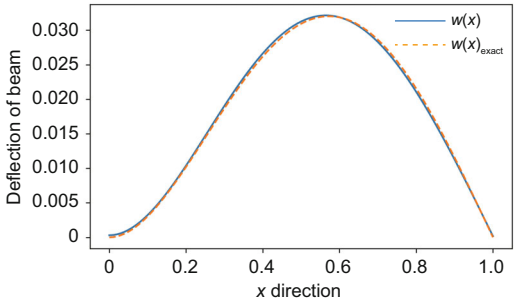

Fig. 5 Comparison of the exact ($w(x)_{\text{exact}}$) (Reddy, 2017) and our predicted ($w(x)$) solution results of residual network with six layers for clamped-simply boundary condition

4 Summary and conclusions

We proposed DEM to study the bending behavior of porous Euler-Bernoulli beams under various boundary conditions and adopted an analytical solution from our previous work to compare the performance of our method. DEM only requires the definition of the potential energy of the system and eliminates the need of a classical discretization, such as finite element method. It can be easily implemented in standard open-source tools such as PyTorch. The objective function, which corresponds to the potential energy of the system plus a term to impose essential boundary conditions, is minimized using the Adam optimizer. We employed tanh as the activation function and determined that an increase in the number of input neurons and blocks in the network structure up to a certain point yields results with acceptable precision and convergence to the exact solution. However, at a certain point, a further increase causes overfitting. Moreover, we determined that the residual network is easier to optimize (with lower computational cost) compared with the fully connected network.

Contributors

Timon RABCZUK devised the project, verified the computational process, and contributed to the final version of the manuscript. Mohammad SALAVATI contributed to the simulation process. Arvin MOJAHEDIN worked out the technical details, performed the computational calculations, and wrote the manuscript.

Conflict of interest

Arvin MOJAHEDIN, Mohammad SALAVATI, and Timon RABCZUK declare that they have no conflict of interest.

References

Alshorbagy AE, Eltaher MA, Mahmoud FF, 2011. Free vibration characteristics of a functionally graded beam by finite element method. *Applied Mathematical Modelling*, 35(1):412-425. https://doi.org/10.1016/j.apm.2010.07.006

Altenbach H, Ochsner A, 2010. Cellular and porous materials in structures and processes. Springer Verlag, Wien, Austria. https://doi.org/10.1007/978-3-7091-0297-8

Anitescu C, Atroshchenko E, Alajlan N, et al., 2019. Artificial neural network methods for the solution of second order boundary value problems. *Computers, Materials & Continua*, 59(1):345-359. https://doi.org/10.32604/cmc.2019.06641

Chakraverty S, Pradhan KK, 2016. Vibration of Functionally Graded Beams and Plates. Academic Press, London, UK, p.33-66. https://doi.org/10.1016/C2015-0-00496-8

Chen D, Yang J, Kitipornchai S, 2016. Free and forced vibrations of shear deformable functionally graded porous beams. *International Journal of Mechanical Sciences*, 108-109:14-22. https://doi.org/10.1016/j.ijmecsci.2016.01.025

Galeban MR, Mojahedin A, Taghavi Y, et al., 2016. Free vibration of functionally graded thin beams made of saturated porous materials. *Steel and Composite Structures*, 21(5):999-1016. https://doi.org/10.12989/scs.2016.21.5.999

Ghannadpour SAM, Mohammadi B, Fazilati J, 2013. Bending, buckling and vibration problems of nonlocal Euler beams using Ritz method. *Composite Structures*, 96:584-589. https://doi.org/10.1016/j.compstruct.2012.08.024

Goodfellow I, Bengio Y, Courville A, 2016. Deep Learning. MIT Press and Cambridge, Cambridge, USA.

Khatir S, Boutchicha D, Le Thanh C, et al., 2020. Improved ANN technique combined with Jaya algorithm for crack identification in plates using XIGA and experimental analysis. *Theoretical and Applied Fracture Mechanics*, 107:102554. https://doi.org/10.1016/j.tafmec.2020.102554

Kingma DP, Jimmy B, 2015. Adam: a Method for Stochastic Optimization. Proceedings of the 3rd International Conference on Learning Representations, p.1-41.

Lagaris IE, Likas A, Fotiadis DI, 1998. Artificial neural networks for solving ordinary and partial differential equations. *IEEE Transactions on Neural Networks*, 9(5):987-1000. https://doi.org/10.1109/72.712178

Li SR, Zhou YH, Zheng XJ, 2002. Thermal post-buckling of a heated elastic rod with pinned-fixed ends. *Journal of Thermal Stresses*, 25(1):45-56. https://doi.org/10.1080/014957302753305862

Liu ZY, Yang YT, Cai QD, 2019. Solving Differential Equation with Constrained Multilayer Feedforward Network. arXiv:1904.06619.

Mojahedin A, Jabbari M, Rabczuk T, 2018. Thermoelastic analysis of functionally graded porous beam. *Journal of Thermal Stresses*, 41(8):937-950. https://doi.org/10.1080/01495739.2018.1446374

Nabian MA, Meidani H, 2018. A Deep Neural Network Surrogate for High-Dimensional Random Partial Differential Equations. arXiv:1806.02957.

Nguyen DK, 2014. Large displacement behaviour of tapered cantilever Euler-Bernoulli beams made of functionally graded material. *Applied Mathematics and Computation*, 237:340-355. https://doi.org/10.1016/j.amc.2014.03.104

Nguyen HX, Nguyen TN, Abdel-Wahab M, et al., 2017. A refined quasi-3D isogeometric analysis for functionally graded microplates based on the modified couple stress theory. *Computer Methods in Applied Mechanics and Engineering*, 313:904-940. https://doi.org/10.1016/j.cma.2016.10.002

Nguyen-Le DH, Tao QB, Nguyen VH, et al., 2020. A data-driven approach based on long short-term memory and hidden Markov model for crack propagation prediction. *Engineering Fracture Mechanics*, 235:107085. https://doi.org/10.1016/j.engfracmech.2020.107085

Phung-Van P, Tran LV, Ferreira AJM, et al., 2017. Nonlinear transient isogeometric analysis of smart piezoelectric functionally graded material plates based on generalized shear deformation theory under thermo-electro-mechanical loads. *Nonlinear Dynamics*, 87(2):879-894. https://doi.org/10.1007/s11071-016-3085-6

Phung-Van P, Thai CH, Nguyen-Xuan H, et al., 2019. Porosity-dependent nonlinear transient responses of functionally graded nanoplates using isogeometric analysis. *Composites Part B: Engineering*, 164(1):215-225. https://doi.org/10.1016/j.compositesb.2018.11.036

Reddy JN, 2017. Energy Principles and Variational Methods in Applied Mechanics, 3rd Edition. John Wiley and Sons, Hoboken, USA.

Sankar BV, 2001. An elasticity solution for functionally graded beams. *Composites Science and Technology*, 64(5):689-696. https://doi.org/10.1016/S0266-3538(01)00007-0

Shirvany Y, Hayati M, Moradian R, 2009. Multilayer perceptron neural networks with novel unsupervised training method for numerical solution of the partial differential equations. *Applied Soft Computing*, 9(1):20-29. https://doi.org/10.1016/j.asoc.2008.02.003

Sirignano J, Spiliopoulos K, 2018. DGM: a deep learning algorithm for solving partial differential equations. *Journal of Computational Physics*, 357:1339-1364. https://doi.org/10.1016/j.jcp.2018.08.029

Thanh CL, Phung-Van P, Thai CH, et al., 2018. Isogeometric analysis of functionally graded carbon nanotube reinforced composite nanoplates using modified couple stress theory. *Composite Structures*, 184:633-649. https://doi.org/10.1016/j.compstruct.2017.10.025

Thanh CL, Tran LV, Bui TQ, et al., 2019. Isogeometric analysis for size-dependent nonlinear thermal stability of porous FG microplates. *Composite Structures*, 221:110838. https://doi.org/10.1016/j.compstruct.2019.04.010

Tran-Ngoc H, Khatir S, de Roeck G, et al., 2019. An efficient artificial neural network for damage detection in bridges and beam-like structures by improving training parameters using cuckoo search algorithm. *Engineering Structures*, 199:109637. https://doi.org/10.1016/j.engstruct.2019.109637

Weinan E, Yu B, 2018. The deep Ritz method: a deep learning-based numerical algorithm for solving variational problems. *Communications in Mathematics and Statistics*, 6(1):1-12. https://doi.org/10.1007/s40304-018-0127-z